Klaus Hermann

Crystallography and Surface Structure

An Introduction
for Surface
Scientists and
Nanoscientists

Klaus Hermann

Crystallography and Surface Structure

Related Titles

Takadoum, J.

Nanomaterials and Surface Engineering

384 pages
Hardcover
ISBN: 978-1-84821-151-3

Kumar, C. S. S. R. (ed.)

Nanostructured Thin Films and Surfaces

451 pages with 186 figures and 4 tables
2010
Hardcover
ISBN: 978-3-527-32155-1

Butt, H.-J., Kappl, M.

Surface and Interfacial Forces

436 pages with 158 figures and 17 tables
2010
Softcover
ISBN: 978-3-527-40849-8

Ertl, G.

Reactions at Solid Surfaces

208 pages
Hardcover
ISBN: 978-0-470-26101-9

Fukumura, H., Irie, M., Iwasawa, Y., Masuhara, H., Uosaki, K. (eds.)

Molecular Nano Dynamics

Vol. I: Spectroscopic Methods and Nanostructures / Vol. II: Active Surfaces, Single Crystals and Single Biocells

740 pages in 2 volumes with approx. 580 figures
2009
Hardcover
ISBN: 978-3-527-32017-2

Förch, R., Schönherr, H., Jenkins, A. T. A. (eds.)

Surface Design: Applications in Bioscience and Nanotechnology

532 pages with 248 figures and 16 tables
2009
Hardcover
ISBN: 978-3-527-40789-7

Klaus Hermann

Crystallography and Surface Structure

An Introduction for Surface Scientists and
Nanoscientists

The Author

Prof. Dr. Klaus Hermann
Fritz Haber Institute
Theory Department
Berlin, Germany

Cover picture
by Klaus Hermann

Contents

Preface

The objective of this book is to provide students and researchers with the foundations of crystallography necessary to understand geometry and symmetry of surfaces and interfaces of crystalline materials. This includes both macroscopic single crystals and crystalline nanoparticles. Knowledge of their geometric properties is a prerequisite for the interpretation of corresponding experimental and theoretical results, which explain both their physical and their chemical behaviors. In particular, surface and interface structure is of vital importance not only for studies of properties near single crystal surfaces but also for research on thin films at solid substrates. Here, technological applications range from semiconductor devices and magnetic storage disks to heterogeneous catalysts.

Crystalline nanoparticles, such as nanotubes, nanowires, or compact particles of finite size, have recently attracted considerable interest due to their novel chemical and physical properties. Examples are carbon nanotubes, silicon nanowires, and nanosize quantum dots at semiconductor surfaces. Although these particles are of finite size in one or more dimensions, their local atom arrangement can still be close to that of extended bulk crystals. In addition, their surfaces and interfaces with other materials can be described analogously to those found for single crystal surfaces. Thus, surface crystallography, covered in this book, can also be applied to analyze geometric properties of nanoparticle surfaces.

While treatises on three-dimensional crystallography are abundant, there are only few chapters on surface crystallography available in specialized surface science reviews. In particular, comprehensive textbooks on surface structure have not yet been published. Nevertheless, students and researchers entering the field need to obtain a thorough overview of surface geometry, which includes all relevant basic crystallographic methods required for theoretical and experimental analyses. This book tries to serve this purpose. It is primarily meant for graduate and PhD students in physics, chemistry, and crystallography and will also help researchers who want to learn in more detail about the geometry at surfaces of single crystals or nanoparticles.

This book is written by a theoretical surface scientist. Therefore, the discussion of methods and approaches in the text is frequently adapted to surfaces and differs at

some places from traditional crystallographic treatment. For example, number theoretical methods are used to derive appropriate transformations between equivalent lattice descriptions. Furthermore, some of the conventional concepts of surface structure are looked at from a different viewpoint and go beyond the standard treatment known inside the surface science community. Examples include the introduction of Miller indices based on netplane-adapted lattices and a thorough mathematical treatment of symmetry, which results in the 17 two-dimensional space groups. Therefore, the text can also be used as a resource complementary to the standard surface science literature.

This book project started as a manuscript of a series of lectures on surface crystallography, given by the author at several international workshops and in universities as well as research institutions where surface science and catalysis groups were engaged in research on structural properties of surfaces. Questions and discussions during the lectures were often the source of more detailed work on different sections of the manuscript and thus helped to improve its presentation. Furthermore, research visits to various surface science groups raised the author's awareness of new or incompletely treated issues to be dealt with. The author is indebted to all those who contributed with their scientific curiosity and criticism. The text has benefited from numerous discussions with surface scientists, crystallographers, and mathematicians of whom only a few are mentioned: Gerhard Ertl, Klaus Heinz, Bernhard Hornfeck, Klaus Müller, John B. Pendry, Gabor A. Somorjai, D. Phil Woodruff. Wolfgang Moritz served as an extremely valuable sparring partner in the world of crystallography. Very special thanks go to Michel A. Van Hove whose constructive criticism, rich ideas, and continuous support during the writing phase were unmatched. Without him the book would not have come out in its present form.

Finally, I am greatly indebted to my wife Hanna for her patience and loving care throughout the time it took to finish this book and beyond.

Fritz Haber Institute, Berlin   *Klaus Hermann*
Summer 2010

1
Introduction

Research in many areas of materials science requires a thorough knowledge of crystalline solid-state systems on an atomic scale. These systems may represent real materials such as complex semiconductors or may act as meaningful models, for example, simulating reactive sites of catalysts. Here, physical and chemical insight depends very much on details of the geometry of local environments around atoms and of possible periodic atom arrangements inside the crystal and at its surface. As examples we mention that

- *chemical binding* between atoms inside a crystal and at its surface strongly depends, apart from atomic parameters, on local geometry [1, 2]. This is very often expressed by local *coordination* describing the number and arrangement of nearest-neighbor atoms with respect to the binding atom. For example, metal atoms in a bulk metal crystal are usually characterized by a large number of nearest neighbors, 8 or 12, yielding metallic binding. At surfaces, the changed chemical binding due to different coordination, compared to that in the bulk, is closely connected with local geometry that can be expressed by relaxation and reconstruction. Furthermore, atoms or molecules can adsorb at specific sites of crystalline substrates, where the adsorption geometry is essential to an understanding of local binding behavior.
- *electronic* properties at surfaces of single crystals can differ substantially from those of the corresponding bulk. For example, the existence of a surface can induce additional electronic states, surface states, that have been found in experiments and studied theoretically some time ago [3]. Here, the detailed surface geometry determines both the existence and the energetic behavior of the states. Further, electronic interband transitions in silicon nanowires and nanodots are found to cause photoluminescence that does not occur in silicon bulk crystals [4]. The difference is explained by both the spatial confinement of the nanoparticles and the changed geometric properties of their atom arrangement. Finally, it has been claimed from experiment that semiconducting bulk silicon shows metallicity at its (7×7) reconstructed $(1\ 1\ 1)$ surface [5], and metallicity is also found in theoretical studies on silicon nanowires [6].

- *magnetism* of crystalline bulk material and its surfaces depends on the crystal structure and local coordination. For example, vanadium sesquioxide (V_2O_3) in its monoclinic crystal structure at low temperatures is antiferromagnetic, whereas its high-temperature phase is described by a trigonal corundum lattice and is paramagnetic [7]. Vanadium crystals with a body-centered cubic lattice are found to be paramagnetic in their bulk volume but ferromagnetic at their surfaces [8]. Other examples are thin iron films grown on top of copper single crystal surfaces where, as a function of film thickness, their crystal geometry changes and, as a consequence, so do their magnetic properties [9].
- *anisotropic electrical conductivity* is often connected with dense atom packing along specific directions inside crystals. An example is given by trigonal $LiCoO_2$ crystals that form the most common lithium storage material for rechargeable batteries. Here, the electrical conductivity is greatly enhanced along densely packed Co and Li planes while it is much smaller perpendicular to the planes [10].
- *catalytic surface reactions* depend crucially on geometric properties of the surfaces of crystalline catalyst materials [11, 12] and are needed for understanding the heterogeneous catalysis at an atomic scale. The atomic surface geometry determines possible adsorption and reaction sites for molecules, which can support specific catalytic reactions but also can exclude others (structure–reactivity relationship [11]). For example, catalytic CO oxidation happens at single crystal surfaces of platinum with different efficiency depending on the surface orientation [13], where the surface geometry determines the type and density of reactive sites.

In addition to bulk crystals and their surfaces, crystalline *nanoparticles* [14, 15] have become a new exciting field of research. This includes nanotubes [16], nanowires [14], or compact particles of finite size, such as atom clusters [17], fullerenes [18], or quantum dots [19], which show novel physical and chemical properties deviating from those of corresponding bulk material. Examples are carbon nanotubes providing substrate material to yield new active catalysts [20] or silicon nanowires whose visible photoluminescence is determined by their size [21]. Furthermore, nanosize quantum dots at semiconductor surfaces are found to yield quite powerful light emitting diodes (LEDs) of technological relevance [19].

These nanosystems are described as *atom aggregates* of finite size in one or more dimensions, where their local geometric arrangement can still be close to that of extended bulk crystals. Likewise, their spatial confinement with corresponding surfaces and interfaces can be considered analogous to that appearing at bulk crystal surfaces. Therefore, surface crystallography, initially developed to describe geometric properties at single crystal surfaces, also forms a sound basis for characterizing geometry of nanoparticle surfaces. This is particularly interesting since the relative number of atoms positioned at nanoparticle surfaces compared to those of their inner volume is always larger than that of extended macroscopic single crystals. Thus, atoms at *nanoparticle surfaces* are expected to play a more important role in determining physical properties than corresponding atoms at single crystal surfaces. In addition, nanoparticles can possess symmetry and geometric properties that do not

appear in single crystals or at their surfaces. Examples are curved nanoparticle surfaces that originate from bending single crystal sections, where in this book *nanotubes* will be discussed as examples.

In many experimental and theoretical studies, real crystalline systems are, for the sake of simplicity, approximately described by *ideal single crystals* with a well-defined atomic composition and an unperturbed three-dimensional periodicity. In addition, surfaces of the single crystals are assumed to be bulk-terminated and of unperturbed two-dimensional periodicity. With this approximation in mind, a rigorous mathematical description of all geometric parameters becomes possible and is one of the basic subjects of classical crystallography. As an illustration, Figure 1.1 shows the geometry of a section of an ideal single crystal of magnesium oxide (MgO) with its perfect three-dimensional periodic arrangement of atoms. Here, sections of ideal planar surfaces, originating from bulk truncation, become visible and demonstrate the variety of surface types for the same crystal depending on the crystal cut.

In this book, we will discuss basic elements and *mathematical methods* used in crystallography to evaluate geometric parameters of single crystals with particular emphasis on their surfaces. We start with ideal bulk crystals of three-dimensional periodicity, where classical bulk crystallography provides a quantitative description. Then, we introduce ideal two-dimensional surfaces as a result of bulk truncation along specific directions including high-density, vicinal, stepped, kinked, and chiral surfaces. We give a detailed account of their two-dimensional symmetry behavior following the crystallographic classification scheme of Bravais lattices and two-
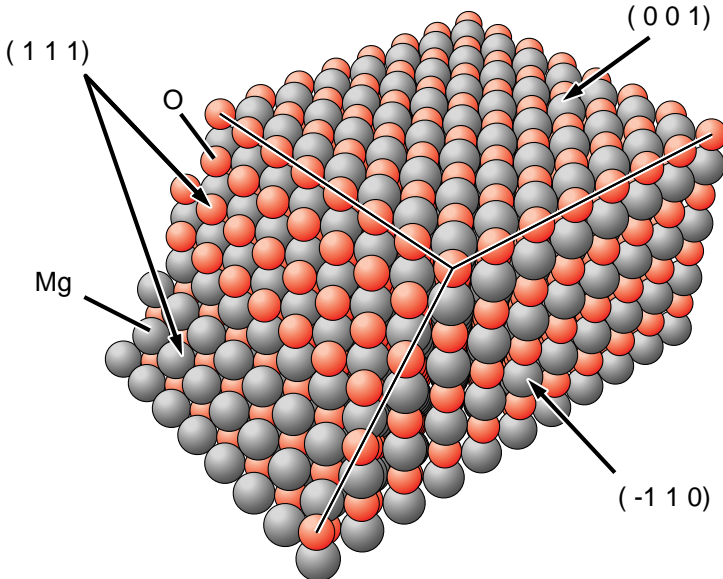
Figure 1.1 Section of an MgO crystal (NaCl lattice). The atoms are shown as colored balls and labeled accordingly. The section is enclosed by nonpolar (0 0 1), (−1 1 0) and by polar (1 1 1) oriented surfaces.

dimensional space groups. Next, we discuss in detail the deviation of atom geometry at surfaces due to changed surface binding compared to the bulk. This is usually described by surface relaxation and reconstruction, where we consider different schemes. After that, we mention crystallographic aspects of commensurate and incommensurate adsorbate systems as special cases of surface reconstruction, where the different notations used in the literature will also be described. The discussion of surface structure will be completed by an overview of the surfaces that have been analyzed quantitatively at an atomic level in scattering, diffraction, imaging, or spectroscopic experiments. Finally, we describe theoretical aspects and structural details of nanotubes of different element composition as special cases of rolled sections of crystal monolayers. These nanotubes are examples of a larger class of crystalline materials, nanoparticles, and demonstrate that crystallographic methods can also be applied to these systems in order to account for their geometric properties. The book concludes with appendices providing details of the mathematical methods used in different chapters.

The theoretical concepts treated in this book will be illustrated by example applications for further understanding, which include results from *measured* real single crystal surfaces that are documented in the NIST Surface Structure Database (SSD) [22–24] or its earlier version SCIS (Surface Crystallographic Information Service) [25]. In addition, each chapter of the book concludes with a set of *exercises*. These exercises are of varying difficulty, ranging from simple problems to small research projects, and are meant to stimulate questions and answers about the different subjects. Some of the exercises may require a *visualization tool* for crystals, such as Balsac [26], or Survis, the visualization part of the SSDIN package [27] or the like.

For the theoretical treatment of some geometric properties of ideal single crystals, we will apply *number theoretical methods*, dealing with relations between integer numbers. While this approach is not commonly used in textbooks on surface science or crystallography, it can considerably simplify the formal treatment. Examples are solutions of linear and quadratic Diophantine equations that facilitate the discussion of netplanes or of atom neighbor shells in crystals. Therefore, number theoretical methods will be introduced briefly as required, and further details are provided in Appendix C.

A few illustrations are included as *stereo pictures* for an enhanced three-dimensional impression. These pictures may be viewed by either using optical stereo glasses (available separately) or by cross-eyed viewing without glasses. In the latter case, viewing for an extended time may overstrain the eyes and should be avoided.

Obviously, the present book cannot cover all aspects of the field and may, in some cases, be quite brief. Furthermore, the selection of topics, as well as their presentation, is, to some degree, determined by the author's personal preferences. However, the interested reader may consult the extensive crystallographic literature, for example, Refs. [28–32], or the solid-state physics literature, for example, Refs. [1, 2], to explore additional details.

2
Bulk Crystals: Three-Dimensional Lattices

This chapter deals with geometric properties of three-dimensional *bulk crystals*, which are described, in their perfect geometry, by atom arrangements that are periodic in three dimensions. For example, Figure 2.1 on the following page shows a section of a (tetragonal) $YBa_2Cu_3O_7$ crystal, where vectors $\underline{R}_1$, $\underline{R}_2$, $\underline{R}_3$ (lattice vectors) indicate the mutually perpendicular directions of periodicity. Furthermore, the basis of the crystal structure consists of 13 atoms ($1 \times$ yttrium, $2 \times$ barium, $3 \times$ copper, $7 \times$ oxygen atoms) in a rectangular block (unit cell) that is repeated periodically inside the crystal. The building unit is shown to the left of the figure.

In this chapter, all *basic definitions* used for a quantitative description of geometric properties of perfect three-dimensional periodic crystals will be provided. Here, the crystals are considered not only in terms of their translational symmetry, that is, periodicity, but also by their different point symmetry elements, such as inversion points, mirror planes, or rotation axes, which determine the positions of all atoms in a crystal. While the definitions and general properties are rather abstract and *mathematical*, they can become quite relevant for theoretical studies of real three-dimensional crystals. For example, lattice representations of crystals are required as input to any electronic structure calculation on solid crystalline material. Furthermore, the theoretical treatment of three-dimensional crystals serves as a safe foundation to study surfaces of single crystals, as will be discussed in Sections 2.4 and 2.5.

2.1
Basic Definitions

The basic definition of a perfect three-dimensional bulk crystal becomes quite clear by considering first a simple example. Figure 2.2a shows a section of the primitive cubic CsCl crystal, which is obviously periodic in three perpendicular directions. Thus, its periodicity can be described by orthogonal vectors $\underline{R}_1$, $\underline{R}_2$, $\underline{R}_3$ (*lattice vectors*), indicated in Figure 2.2b, whose lengths define corresponding periodicity lengths. The lattice vectors span a cubic cell (*morphological unit cell*) that contains one cesium and chlorine atom each at positions given by vectors $\underline{r}_1$ (Cs), $\underline{r}_2$ (Cl) (*lattice basis vectors*)
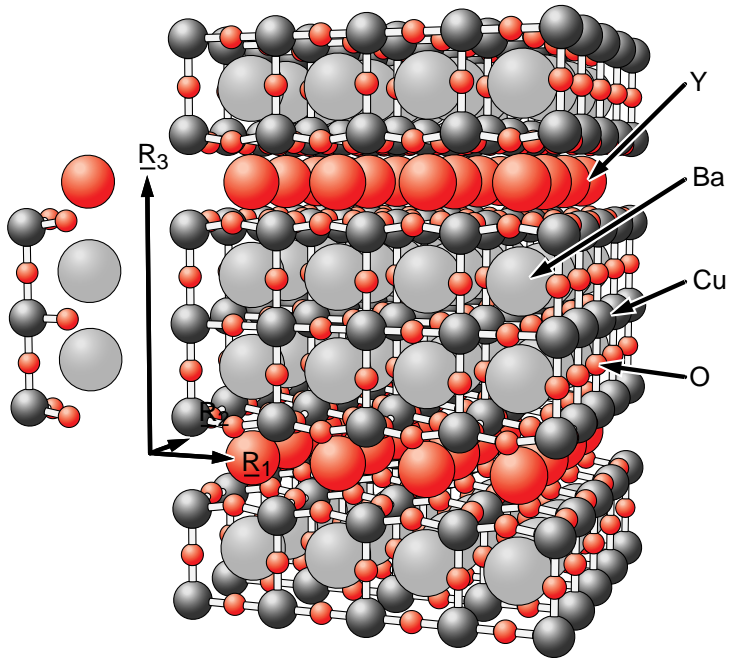
Figure 2.1 Section of a tetragonal $YBa_2Cu_3O_7$ crystal. The atoms are shown as colored balls and labeled accordingly. In addition, the basis of 13 atoms in a rectangular cell and lattice vectors $\underline{R}_1$, $\underline{R}_2$, $\underline{R}_3$ are included to the left.
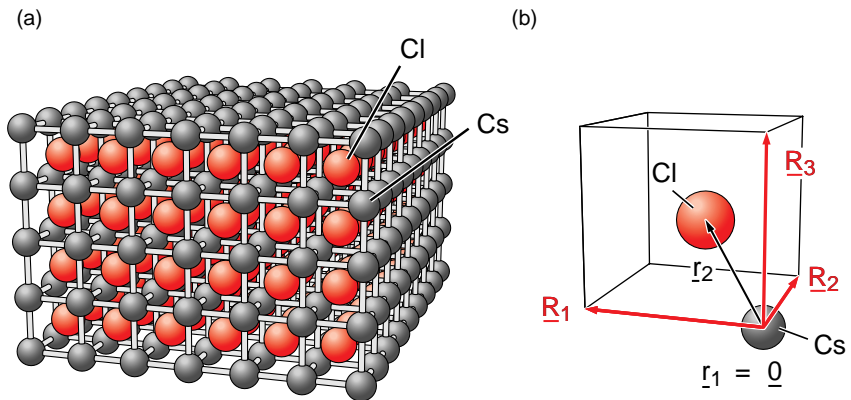
Figure 2.2 (a) Section of a primitive cubic CsCl crystal. Sticks connect neighboring Cs atoms to indicate the crystal geometry. (b) Primitive morphological unit cell with two atoms, Cs and Cl (see text). The atoms are identical to those labeled in (a). Both the lattice vectors $\underline{R}_1$, $\underline{R}_2$, $\underline{R}_3$ and the lattice basis vectors, $\underline{r}_1 = \underline{0}$ for Cs and $\underline{r}_2$ for Cl, are shown and labeled accordingly.
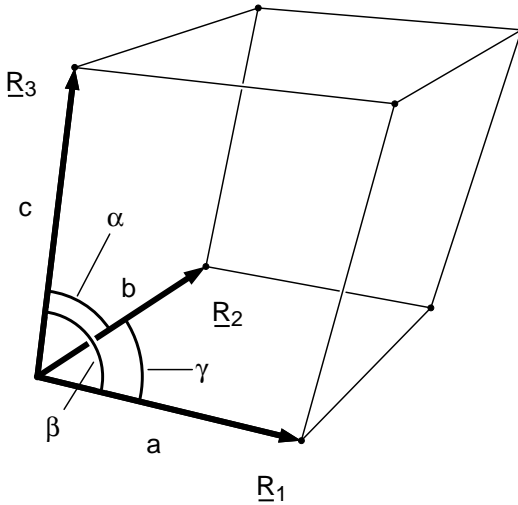
Figure 2.3   Definition of crystallographic lattice parameters a, b, c, α, β, γ (see text).

(Figure 2.2b). Obviously, a periodic repetition of the unit cell along $\underline{R}_1$, $\underline{R}_2$, $\underline{R}_3$ can be used to build the complete infinite crystal.

In the general case, the formal definition of a perfect three-dimensional bulk *crystal* starts from a three-dimensional periodic arrangement of atoms. Here, the crystal periodicity is described by a *lattice* with lattice vectors $\underline{R}_1$, $\underline{R}_2$, $\underline{R}_3$. Thus, the lattice forms an infinite and periodic array of *lattice points* reached from a common origin by vectors $\underline{R}$ with

$$\underline{R} = n_1\,\underline{R}_1 + n_2\,\underline{R}_2 + n_3\,\underline{R}_3 \tag{2.1}$$

where the coefficients n_1, n_2, n_3 can assume any integer value. This means, in particular, that each lattice point experiences the same environment created by all other points.

The lattice vectors can be given in different ways, where the choice depends on the type of application. While for numerical calculations it may be preferable to define $\underline{R}_1$, $\underline{R}_2$, $\underline{R}_3$ with respect to an absolute *Cartesian coordinate system* as

$$\underline{R}_i = (x_i, y_i, z_i), \quad i = 1, 2, 3 \tag{2.2}$$

it is common in the crystallographic literature to define these vectors by *lattice parameters* describing their lengths (*lattice constants*) a, b, c and by their mutual *angles* α, β, γ, as sketched in Figure 2.3, where

$$a = |\underline{R}_1|, \quad b = |\underline{R}_2|, \quad c = |\underline{R}_3| \tag{2.3a}$$

$$\underline{R}_1 \cdot \underline{R}_2 = a\,b\cos(\gamma), \quad \underline{R}_1 \cdot \underline{R}_3 = a\,c\cos(\beta), \quad \underline{R}_2 \cdot \underline{R}_3 = b\,c\cos(\alpha) \tag{2.3b}$$

Examples are given by lattices denoted as

$$simple\ cubic, \quad where \quad a = b = c, \quad \alpha = \beta = \gamma = 90° \tag{2.4}$$

$$hexagonal, \quad where \quad a = b \neq c, \quad \alpha = \beta = 90°, \gamma = 120° \tag{2.5}$$

Relations (2.3a) and (2.3b) can be *inverted* to yield lattice vectors in Cartesian coordinates starting from the six parameters, a, b, c, and α, β, γ, given in (2.3a) and (2.3b), where one possible inversion is

$$\underline{R}_1 = a(1, 0, 0), \quad \underline{R}_2 = b(\cos(\gamma), \sin(\gamma), 0)$$
$$\underline{R}_3 = c(\cos(\beta), (\cos(\alpha) - \cos(\beta)\cos(\gamma))/\sin(\gamma), v_3/\sin(\gamma)) \tag{2.6a}$$

with

$$v_3 = \{(\cos(\beta - \gamma) - \cos(\alpha))(\cos(\alpha) - \cos(\beta + \gamma))\}^{1/2} \tag{2.6b}$$

This yields for simple cubic (sc) lattices with (2.4)

$$\underline{R}_1 = a(1, 0, 0), \quad \underline{R}_2 = a(0, 1, 0), \quad \underline{R}_3 = a(0, 0, 1) \tag{2.7}$$

and for hexagonal lattices with (2.5)

$$\underline{R}_1 = a(1, 0, 0), \quad \underline{R}_2 = a(-1/2, \sqrt{3}/2, 0), \quad \underline{R}_3 = c(0, 0, 1) \tag{2.8}$$

The lattice vectors $\underline{R}_1$, $\underline{R}_2$, $\underline{R}_3$ span a six-faced polyhedron (the so-called parallelepiped), defining the *morphological unit cell*, often referred to as the *unit cell*, whose edges are parallel to $\underline{R}_1$, $\underline{R}_2$, $\underline{R}_3$ and whose volume V_{el} is given by

$$V_{el} = |(\underline{R}_1 \times \underline{R}_2)\,\underline{R}_3| \tag{2.9}$$

The unit cell is called *primitive unit cell* if its volume is the smallest of all possible unit cells in the crystal. This is equivalent to requiring that there is no additional lattice point, described by vector $\underline{R}'$ with

$$\underline{R}' = \kappa_1\,\underline{R}_1 + \kappa_2\,\underline{R}_2 + \kappa_3\,\underline{R}_3, \quad 0 \leq \kappa_i < 1 \tag{2.10}$$

inside the morphological unit cell of the lattice. Otherwise, the cell is *nonprimitive* and there must also be lattice points $\underline{R}'$ inside the unit cell. Analogously, lattice vectors $\underline{R}_1$, $\underline{R}_2$, $\underline{R}_3$ whose morphological unit cell is primitive are called *primitive lattice vectors*, otherwise *nonprimitive*. For example, both the cubic unit cell of CsCl and the corresponding lattice vectors, shown in Figure 2.2, are primitive. On the other hand, replacing all cesium and chlorine atoms in Figure 2.2 by one atom type, for example, iron, yields a body-centered cubic crystal. Here, the lattice vectors $\underline{R}_1$, $\underline{R}_2$, $\underline{R}_3$, shown in the figure, are nonprimitive since vector $\underline{r}_2$ now becomes a lattice vector in the morphological unit cell.

In a crystal, the morphological unit cell contains in general p atoms at positions given by vectors $\underline{r}_1$, ..., $\underline{r}_p$ (lattice basis vectors) that form the *basis* of the crystal structure (the basis is sometimes also called the *structure*). Each atom at $\underline{r}_i$ carries a *label* characterizing its properties, such as its nuclear charge or element name. These

labels, usually omitted in the following, will be attached to each lattice basis vector if needed. For example, a definition $\underline{r}_3^{Cl}$ would refer to a chlorine atom placed at a position given by the third lattice basis vector. All lattice basis vectors $\underline{r}_i$ in the morphological unit cell can be written as *linear combinations* of the lattice vectors $\underline{R}_1$, $\underline{R}_2$, $\underline{R}_3$, that is,

$$\underline{r}_i = x_i\,\underline{R}_1 + y_i\,\underline{R}_2 + z_i\,\underline{R}_3, \quad i = 1, \ldots, p \tag{2.11}$$

where x_i, y_i, z_i are real-valued coefficients with $|x_i| < 1$, $|y_i| < 1$, $|z_i| < 1$. This use of *relative coordinates* x_i, y_i, z_i to describe atoms in the unit cell is common practice in the crystallographic literature [28, 32]. According to definition (2.11), the coefficients x_i, y_i, z_i are in general not connected with the Cartesian coordinate system but with coordinate axes given by the lattice vectors $\underline{R}_1$, $\underline{R}_2$, $\underline{R}_3$.

The *origin* of the morphological unit cell in a crystal can always be chosen freely since the complete infinite crystal consists of a periodic arrangement of unit cells in three dimensions. In particular, the origin does not need to coincide with a specific atom position, as considered in the example of CsCl above. However, it is usually chosen in such manner as to maximize the number of point symmetry elements, such as inversion points, mirror planes, or rotation axes, which are determined by the lattice vectors $\underline{R}_1$, $\underline{R}_2$, $\underline{R}_3$ together with the lattice basis vectors $\underline{r}_1, \ldots, \underline{r}_p$. This will be discussed in greater detail in Section 2.4.

Altogether, a *crystal* is characterized uniquely by its *lattice* defined by lattice vectors $\underline{R}_1$, $\underline{R}_2$, $\underline{R}_3$ and its *basis* defined by lattice basis vectors $\underline{r}_1, \ldots, \underline{r}_p$. Thus, general atom positions in the crystal can be given by

$$\underline{r} = n_1\,\underline{R}_1 + n_2\,\underline{R}_2 + n_3\,\underline{R}_3 + \underline{r}_i \tag{2.12}$$

where the coefficients n_1, n_2, n_3 can assume any integer value and index $i = 1, \ldots, p$ counts the number of atoms in the unit cell. Here, the lattice and the basis can be treated as *separate* elements of a crystal structure (which are only connected by the symmetry elements as will be discussed in Section 2.4). This will be emphasized in the following Section 2.2.

2.2
Representation of Bulk Crystals

There is one important aspect that governs all formal descriptions of crystal structures, the fact that descriptions of crystals are *not unique*. This means that, for a given definition of a crystal, one can always find an infinite number of alternatives that describe the same crystal. While this ambiguity may be considered a drawback at first glance, it allows choosing crystal representations according to additional constraints, for example, those given by symmetry, physical, or chemical properties. Here, one can distinguish between alternative descriptions that affect the crystal basis but not its lattice representation and those where both the lattice representation and the basis are affected.

2.2.1
Alternative Descriptions Conserving the Lattice Representation

Examples of alternative crystal descriptions that do not affect the crystal lattice are given by elemental or compound *decompositions* of a crystal. Here, the basic idea is to decompose the basis of the unit cell of a complex crystal into components and consider (fictitious) crystals of these components with the same periodicity as that of the initial crystal, given by its lattice. This decomposition is not only of didactic value but may also help to understand details of chemical binding in the crystal. In the simplest case, a crystal with p atoms in its primitive unit cell can be considered alternatively as a superposition of p crystals of the same lattice but only one atom in their primitive unit cells. The origins of the corresponding p crystals can be set at positions given by the lattice basis vectors $\underline{r}_i$ of the initial crystal.

As very simple example, the primitive cubic cesium chloride (CsCl) crystal, shown in Figure 2.2, is defined by a lattice with lattice vectors $\underline{R}_1$, $\underline{R}_2$, $\underline{R}_3$ given by (2.7). Furthermore, its basis includes two atoms, Cs and Cl, which can be positioned at

$$\underline{r}_1 = a\,(0,0,0) \text{ for Cs}, \quad \underline{r}_2 = a\,(1/2,1/2,1/2) \text{ for Cl} \tag{2.13}$$

with a denoting the lattice constant of CsCl. Thus, the crystal can be considered a superposition of two primitive cubic monoatomic crystals, one for cesium and one for chlorine, where their origins are shifted by $\pm(\underline{r}_2 - \underline{r}_1) = \pm\,a\,(1/2, 1/2, 1/2)$ with respect to each other.

A more complex example is the tetragonal $YBa_2Cu_3O_7$ crystal, shown in Figure 2.1. Here, the lattice vectors can be written in Cartesian coordinates as

$$\underline{R}_1 = a(1,0,0), \quad \underline{R}_2 = a(0,1,0), \quad \underline{R}_3 = c(0,0,1) \tag{2.14a}$$

and the morphological unit cell contains 13 atoms resulting in 13 lattice basis vectors $\underline{r}_i$ with

$$
\begin{aligned}
&\text{Y atom}: \quad \underline{r}_1 = (1/2, 1/2, 5/6) \\
&\text{Ba atoms}: \underline{r}_2 = (1/2, 1/2, 1/6), \quad \underline{r}_3 = (1/2, 1/2, 1/2) \\
&\text{Cu atoms}: \underline{r}_4 = (0,0,0), \qquad\quad \underline{r}_5 = (0,0,1/3), \qquad \underline{r}_6 = (0,0,2/3) \\
&\text{O atoms}: \underline{r}_7 = (1/2, 0, -\varepsilon), \qquad \underline{r}_8 = (0, 1/2, -\varepsilon), \quad \underline{r}_9 = (0,0,1/6), \\
&\qquad\quad \underline{r}_{10} = (0, 1/2, 1/3), \qquad \underline{r}_{11} = (0,0,1/2), \qquad \underline{r}_{12} = (1/2, 0, 2/3 + \varepsilon), \\
&\qquad\quad \underline{r}_{13} = (0, 1/2, 2/3 + \varepsilon)
\end{aligned}
$$

$$\tag{2.14b}$$

using relative coordinates (2.11). Experiments yield a relative position shift ε of four oxygen atoms of $\varepsilon = 0.026$. Obviously, this crystal can be conceptually decomposed into 13 monoatomic (tetragonal) crystals, 1 yttrium, 2 barium, 3 copper, and 7 oxygen crystals.

Alternatively, one can decompose the $YBa_2Cu_3O_7$ crystal into physically more meaningful subunits that include *several* of the atoms of the initial unit cell. For example, Figure 2.4 illustrates a decomposition of the $YBa_2Cu_3O_7$ crystal into its

YBa$_2$Cu$_3$O$_7$ Cu$_3$O$_7$ YBa$_2$

Y

Ba

Cu

O

(a)   (b)   (c)
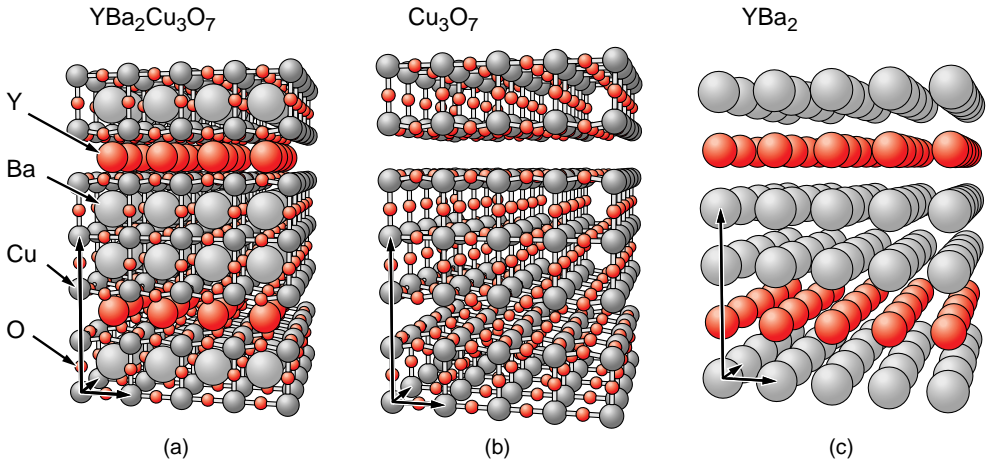
Figure 2.4 Decomposition of the YBa$_2$Cu$_3$O$_7$ crystal (a) into its copper oxide (b) and heavy metal components (c). The component crystals are denoted as Cu$_3$O$_7$ and YBa$_2$, respectively. Atoms are shown as colored balls and labeled accordingly. In addition, the lattice vectors $\underline{R}_1$, $\underline{R}_2$, $\underline{R}_3$ are indicated by arrows.

copper oxide and its heavy metal components, denoted Cu$_3$O$_7$ and YBa$_2$, respectively, in Figure 2.4. Here, the unit cells of the component crystals contain 10 and 3 atoms each, where the Cu$_3$O$_7$ component is believed to contribute to the high-temperature superconductivity of YBa$_2$Cu$_3$O$_7$.

A very illustrative example of crystal decomposition is given by the *diamond* crystal, shown in Figure 2.5. Its lattice can be defined as a simple cubic lattice where lattice
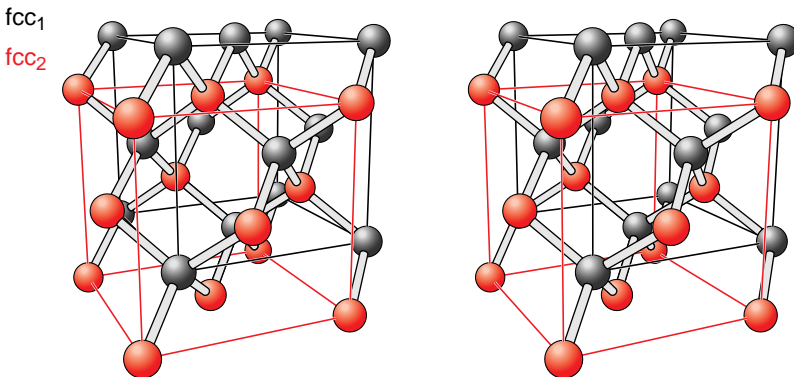
fcc$_1$
fcc$_2$

Figure 2.5 Decomposition of the diamond crystal into two (shifted) face-centered cubic crystals, denoted fcc$_1$ (gray balls, black lines) and fcc$_2$ (red balls and red lines), as given in the legend to the left. The crystal is displayed by a stereo picture where the visual three-dimensional impression is obtained by cross-eyed viewing.

vectors are given by (2.7). The basis of the crystal includes eight carbon atoms in tetrahedral arrangements resulting in eight lattice basis vectors $\underline{r}_i$ with

$$\underline{r}_1 = (0, 0, 0), \qquad \underline{r}_2 = (0, 1/2, 1/2), \quad \underline{r}_3 = (1/2, 0, 1/2),$$

$$\underline{r}_4 = (1/2, 1/2, 0), \quad \underline{r}_5 = (1/4, 1/4, 1/4), \; \underline{r}_6 = (1/4, 3/4, 3/4), \tag{2.15}$$

$$\underline{r}_7 = (3/4, 1/4, 3/4), \; \underline{r}_8 = (3/4, 3/4, 1/4)$$

in relative coordinates (2.11). This shows, first, that the diamond crystal can be decomposed into eight simple cubic (sc) crystals, each with one carbon in the primitive unit cell. Obviously, the lattice basis vectors $\underline{r}_5$, $\underline{r}_6$, $\underline{r}_7$, $\underline{r}_8$ arise from $\underline{r}_1$, $\underline{r}_2$, $\underline{r}_3$, $\underline{r}_4$ by identical shifts with

$$\underline{r}_{i+4} = \underline{r}_i + 1/4(1, 1, 1), \quad i = 1, 2, 3, 4 \tag{2.16}$$

This suggests that the diamond crystal can also be decomposed into two identical simple cubic crystals with four atoms in their unit cells each, where the origins of the two crystals are shifted by a vector 1/4 (1, 1, 1) with respect to each other. The lattices of the two component crystals will be shown in Section 2.2.2 to be identical with face-centered cubic (fcc) lattices. Thus, the diamond crystal can be alternatively described by a superposition of two fcc crystals. This becomes obvious by an inspection of Figure 2.5.

2.2.2
Alternative Descriptions Affecting the Lattice Representation

There are many possibilities of alternative descriptions of crystals where their lattices are represented differently. These alternatives may not only be preferred because of *conceptual* convenience but may also be required due to *computational* necessity. For example, many researchers in the surface science community (and not only there) find it convenient to think in terms of Cartesian coordinates, using orthogonal unit vectors in three-dimensional space. Therefore, they prefer to characterize lattices, if possible, by orthogonal lattice vectors $\underline{R}_1$, $\underline{R}_2$, $\underline{R}_3$ even though they have to consider corresponding crystal bases with a larger number of atoms. This will be discussed for body- and face-centered cubic lattices in Section 2.2.2.1.

Theoretical studies on extended geometric perturbations in a crystal, such as those originating from imperfections or stress, often require to consider unit cells and lattice vectors $\underline{R}'_1$, $\underline{R}'_2$, $\underline{R}'_3$ that are larger than those, $\underline{R}_1$, $\underline{R}_2$, $\underline{R}_3$, of the unperturbed crystal. Here, a direct computational comparison of results for the perturbed crystal with those for the unperturbed crystal often suggests applying the same (enlarged) lattice vectors $\underline{R}'_1$, $\underline{R}'_2$, $\underline{R}'_3$ to both systems. As a result, the unperturbed crystal is described by a lattice with a larger unit cell and an appropriately increased number of atoms in the unit cell. This is the basic idea behind so-called *superlattice* methods that will be discussed in Section 2.2.2.2.

Ideal single crystal surfaces, which originate from bulk truncation yielding two-dimensional periodicity at the surface, will be treated in detail in Chapter 4. Here, the

analysis of geometric properties at the surface can be facilitated greatly by using so-called *netplane-adapted* lattice vectors $\underline{R}'_1, \underline{R}'_2, \underline{R}'_3$. These are given by linear transformations of the initial bulk lattice vectors, where the shape of the morphological unit cell may change, but neither its volume nor the number of atoms in the cell. Clearly, differently oriented surfaces require different sets of netplane-adapted lattice vectors leading to many alternative descriptions of the bulk lattice, as discussed in Section 2.2.2.3.

2.2.2.1 Cubic, Hexagonal, and Trigonal Lattices

The family of cubic lattices – simple, body-centered, and face-centered cubic – are closely connected with each other, which is why many scientists use the simplest of the three, the *simple cubic* lattice as their usual reference. This lattice, also called *cubic-P* and often abbreviated by *sc* is described in Cartesian coordinates by lattice vectors

$$\underline{R}_1^{sc} = a\,(1,0,0), \quad \underline{R}_2^{sc} = a\,(0,1,0), \quad \underline{R}_3^{sc} = a\,(0,0,1) \tag{2.17}$$

with three mutually orthogonal vectors of equal length, given by the lattice constant a.

The *body-centered cubic* lattice, also called *I-centered* or *cubic-I* and often abbreviated by *bcc* (Figure 2.6), can be defined in Cartesian coordinates by lattice vectors

$$\underline{R}_1 = a/2(-1,1,1), \quad \underline{R}_2 = a/2(1,-1,1), \quad \underline{R}_3 = a/2(1,1,-1) \tag{2.18}$$

Here, the three vectors are still of the same length

$$|\underline{R}_1| = |\underline{R}_2| = |\underline{R}_3| = (\sqrt{3}/2)a \tag{2.19}$$
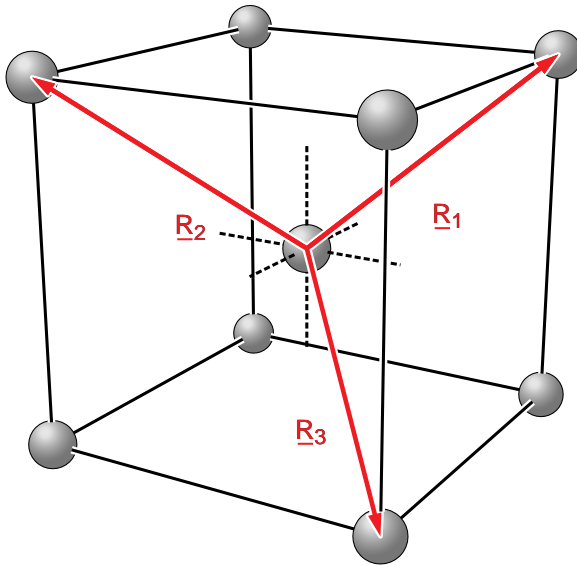
Figure 2.6 Lattice vectors $\underline{R}_1, \underline{R}_1, \underline{R}_1$ of the body-centered cubic (bcc) lattice sketched inside a cubic frame and labeled accordingly (see text). Atoms of the corresponding bcc crystal are shown as balls.

but they are not orthogonal to each other, forming angles $\alpha = \beta = \gamma = 109.47°$ ($\cos \alpha = -1/3$) according to (2.3b). *General lattice points* of the bcc lattice are given in Cartesian coordinates by vectors

$$\underline{R} = n_1 \underline{R}_1 + n_2 \underline{R}_2 + n_3 \underline{R}_3 = a/2(-n_1 + n_2 + n_3, n_1 - n_2 + n_3, n_1 + n_2 - n_3)$$
$$= a/2(N_1, N_2, N_3), \quad n_1, n_2, n_3, N_1, N_2, N_3 \text{ integer} \tag{2.20}$$

where the integers n_1, n_2, n_3 and N_1, N_2, N_3 are connected by

$$N_1 = -n_1 + n_2 + n_3, \quad N_2 = n_1 - n_2 + n_3, \quad N_3 = n_1 + n_2 - n_3 \tag{2.21}$$

Relation (2.20) together with the definition of the simple cubic lattice vectors can be written as

$$\underline{R} = n_1 \underline{R}_1 + n_2 \underline{R}_2 + n_3 \underline{R}_3 = 1/2(N_1 \underline{R}_1^{sc} + N_2 \underline{R}_2^{sc} + N_3 \underline{R}_3^{sc}) \tag{2.22}$$

which demonstrates the connection between the body-centered and the simple cubic lattices. While the integer coefficients n_1, n_2, n_3 can be freely chosen, the integer coefficients N_1, N_2, N_3 are not independent. Relations (2.21) yield

$$N_2 = N_1 + 2(n_1 - n_2), \quad N_3 = N_1 + 2(n_1 - n_3) \tag{2.23}$$

Hence, the integers N_1, N_2, N_3 can only be all odd or all even for any choice of n_1, n_2, n_3.

If N_1, N_2, N_3 in (2.20) are *all even*, that is, they can be represented by

$$N_i = 2 m_i, \quad i = 1, 2, 3 \quad \text{for any integer } m_i \tag{2.24}$$

then relation (2.22) together with (2.24) leads to

$$\underline{R} = m_1 \underline{R}_1^{sc} + m_2 \underline{R}_2^{sc} + m_3 \underline{R}_3^{sc}, \quad m_1, m_2, m_3 \text{ integer} \tag{2.25}$$

which describes a simple cubic lattice as one subset of the bcc lattice.

If, on the other hand, N_1, N_2, N_3 in (2.20) are *all odd*, that is, they can be represented by

$$N_i = 2 m_i + 1, \quad i = 1, 2, 3 \text{ for any integer } m_i \tag{2.26}$$

then relation (2.22) together with (2.26) leads to

$$\underline{R} = m_1 \underline{R}_1^{sc} + m_2 \underline{R}_2^{sc} + m_3 \underline{R}_3^{sc} + \underline{v}, \quad m_1, m_2, m_3 \text{ integer} \tag{2.27}$$

with

$$\underline{v} = 1/2(\underline{R}_1^{sc} + \underline{R}_2^{sc} + \underline{R}_3^{sc}) \tag{2.28}$$

This also describes a simple cubic lattice as the second subset of the bcc lattice, where the second sc lattice is, however, shifted by a vector $\underline{v}$ with respect to the first. Thus, the constraints for N_1, N_2, N_3 in (2.21) yield a decomposition of the bcc lattice into *two* identical sc lattices that are shifted with respect to each other by vector $\underline{v}$ of (2.28). The two sc lattices are sketched in Figure 2.7 and denoted sc$_1$ and sc$_2$.

As a consequence, any crystal with a bcc lattice given by lattice vectors (2.18) can be alternatively described by a crystal with a simple cubic lattice with lattice vectors (2.17), where the unit cell of the sc lattice contains twice as many atoms
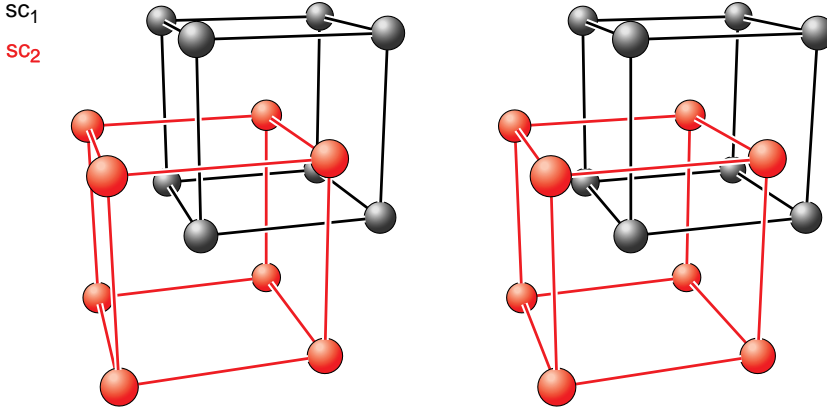
Figure 2.7 Visual decomposition of the body-centered cubic crystal into two (shifted) simple cubic crystals, denoted sc$_1$ (gray balls and black lines) and sc$_2$ (red balls and red lines), as given in the legend to the left. The crystal is displayed by a stereo picture where the visual three-dimensional impression is obtained by cross-eyed viewing.

with atom pairs separated by vector $\underline{v}$. Furthermore, the lattice vectors $\underline{R}_1^{sc}, \underline{R}_2^{sc}, \underline{R}_3^{sc}$ of the sc lattice representation are *nonprimitive* since vector

$$\underline{v} = 1/2(\underline{R}_1^{sc} + \underline{R}_2^{sc} + \underline{R}_3^{sc}) = \underline{R}_1 + \underline{R}_2 + \underline{R}_3 \tag{2.29}$$

according to (2.18) is a true lattice vector.

The *face-centered cubic* lattice, also called *F-centered* or *cubic-F* and often abbreviated by *fcc* (Figure 2.8), can be defined in Cartesian coordinates by lattice vectors

$$\underline{R}_1 = a/2(0, 1, 1), \quad \underline{R}_2 = a/2(1, 0, 1), \quad \underline{R}_3 = a/2(1, 1, 0) \tag{2.30}$$

Here, the three vectors are also of the same length

$$|\underline{R}_1| = |\underline{R}_2| = |\underline{R}_3| = a/\sqrt{2} \tag{2.31}$$

but not orthogonal to each other, forming angles $\alpha = \beta = \gamma = 60°$ (cos $\alpha = 1/2$) according to (2.3b). *General lattice points* of the fcc lattice are given in Cartesian coordinates by vectors

$$\underline{R} = n_1 \underline{R}_1 + n_2 \underline{R}_2 + n_3 \underline{R}_3 = a/2(n_2 + n_3, n_1 + n_3, n_1 + n_2)$$
$$= a/2(N_1, N_2, N_3), \quad n_1, n_2, n_3, N_1, N_2, N_3 \text{ integer} \tag{2.32}$$

where the integers n_1, n_2, n_3 and N_1, N_2, N_3 are connected by

$$N_1 = n_2 + n_3, \quad N_2 = n_1 + n_3, \quad N_3 = n_1 + n_2 \tag{2.33}$$

Relation (2.32) together with the definition of the simple cubic lattice vectors can be written as

$$\underline{R} = n_1 \underline{R}_1 + n_2 \underline{R}_2 + n_3 \underline{R}_3 = 1/2(N_1 \underline{R}_1^{sc} + N_2 \underline{R}_2^{sc} + N_3 \underline{R}_3^{sc}) \tag{2.34}$$
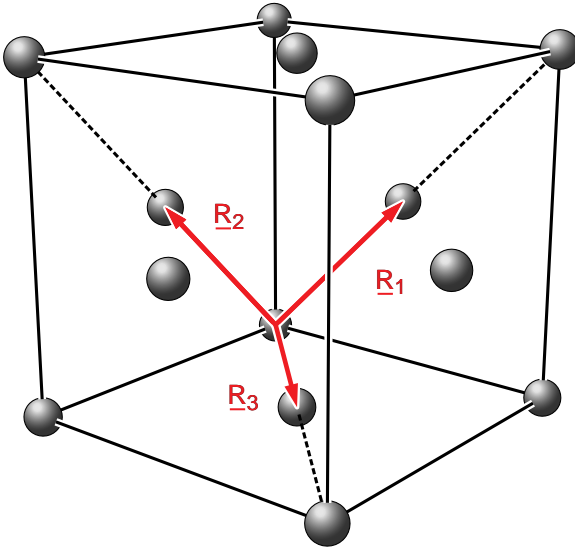
Figure 2.8 Lattice vectors $\underline{R}_1, \underline{R}_1, \underline{R}_1$ of the face-centered cubic (fcc) lattice sketched in a cubic frame and labeled accordingly (see text). Atoms of the corresponding fcc crystal are shown as balls. The dashed lines are meant to assist the visual orientation in the figure.

which shows the connection between the face-centered and the simple cubic lattices. As in the bcc case, the integer coefficients N_1, N_2, N_3 are not independent. Even- and odd-valued combinations of the initial coefficients n_1, n_2, n_3 yield eight cases as shown in Table 2.1.

As a result, integers N_1, N_2, N_3 reduce to *four* different types of *even/odd combinations*:

(a) $N_i = 2\,m_i$, $i = 1$, 2, 3 (cases 1 and 2 in Table 2.1), which results, according to (2.34), in

$$\underline{R} = a/2(N_1, N_2, N_3) = a(m_1, m_2, m_3), \quad m_1, m_2, m_3 \text{ integer} \tag{2.35a}$$

Table 2.1 List of all possible even/odd integer combinations N_1, N_2, N_3 following from even/odd integer combinations n_1, n_2, n_3 according to Equation 2.33.

Case	n_1	n_2	n_3	N_1	N_2	N_3
1	e	e	e	e	e	e
2	o	o	o	e	e	e
3	o	e	e	e	o	o
4	e	o	o	e	o	o
5	e	o	e	o	e	o
6	o	e	o	o	e	o
7	e	e	o	o	o	e
8	o	o	e	o	o	e

Characters *e* and *o* stand for even and odd integers, respectively.

describing the simple cubic lattice given by (2.27) with its origin coinciding with that of the fcc lattice, corresponding to an origin shift $\underline{v}_1 = \underline{0}$ (see below).

(b) $N_1 = 2\,m_1,\ N_2 = 2\,m_2 + 1,\ N_3 = 2\,m_3 + 1$ (cases 3 and 4), resulting in

$$\underline{R} = a/2(N_1, N_2, N_3) = a(m_1, m_2, m_3) + \underline{v}_2$$
$$\underline{v}_2 = 1/2(\underline{R}_2^{sc} + \underline{R}_3^{sc}) \tag{2.35b}$$

describing the sc lattice for an origin shift $\underline{v}_2$.

(c) $N_1 = 2\,m_1 + 1,\ N_2 = 2\,m_2,\ N_3 = 2\,m_3 + 1$ (cases 5 and 6), resulting in

$$\underline{R} = a/2(N_1, N_2, N_3) = a(m_1, m_2, m_3) + \underline{v}_3$$
$$\underline{v}_3 = 1/2(\underline{R}_1^{sc} + \underline{R}_3^{sc}) \tag{2.35c}$$

describing the sc lattice for an origin shift $\underline{v}_3$.

(d) $N_1 = 2\,m_1 + 1,\ N_2 = 2\,m_2 + 1,\ N_3 = 2\,m_3$ (cases 7 and 8), resulting in

$$\underline{R} = a/2(N_1, N_2, N_3) = a(m_1, m_2, m_3) + \underline{v}_4$$
$$\underline{v}_4 = 1/2(\underline{R}_1^{sc} + \underline{R}_2^{sc}) \tag{2.35d}$$

describing the sc lattice for an origin shift $\underline{v}_4$.

Therefore, the constraints for N_1, N_2, N_3 in (2.33) yield a decomposition of the fcc lattice into *four* identical sc lattices that are shifted with respect to each other according to their origins at $\underline{v}_1$, $\underline{v}_2$, $\underline{v}_3$, $\underline{v}_4$ of (2.35a)–(2.35d). The four sc lattices are sketched in Figure 2.9 and denoted sc_1 to sc_4.
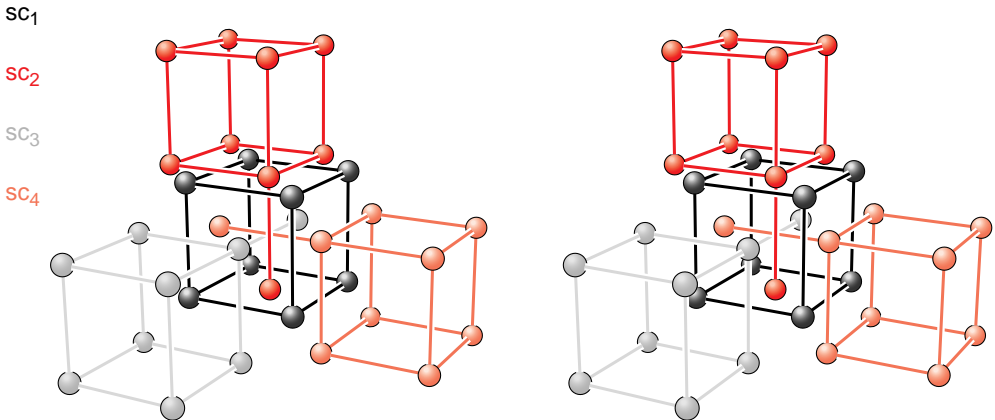
Figure 2.9 Visual decomposition of the fcc crystal into four (shifted) sc crystals, denoted sc_1 (dark gray balls and black lines), sc_2 (dark red balls and lines), sc_3 (light gray balls and lines), and sc_4 (light red balls and lines), as given in the legend to the left. The crystal is displayed by a stereo picture where the visual three-dimensional impression is obtained by cross-eyed viewing.

Consequently, any crystal with an fcc lattice given by lattice vectors (2.30) can be alternatively described by a crystal with an sc lattice with lattice vectors (2.17), where the unit cell of the sc lattice contains four times as many atoms with atom pairs separated by vectors $\underline{v}_i - \underline{v}_j$, $i, j = 1, \ldots, 4$. Furthermore, the lattice vectors $\underline{R}_1^{sc}$, $\underline{R}_2^{sc}$, $\underline{R}_3^{sc}$ of the sc lattice representation are *nonprimitive* since the four vectors $\underline{v}_i$

$$\underline{v}_1 = 0 \tag{2.36a}$$

$$\underline{v}_2 = 1/2(\underline{R}_2^{sc} + \underline{R}_3^{sc}) = \underline{R}_1 \tag{2.36b}$$

$$\underline{v}_3 = 1/2(\underline{R}_1^{sc} + \underline{R}_3^{sc}) = \underline{R}_2 \tag{2.36c}$$

$$\underline{v}_4 = 1/2(\underline{R}_1^{sc} + \underline{R}_2^{sc}) = \underline{R}_3 \tag{2.36d}$$

according to (2.30) are true lattice vectors.

The *hexagonal* lattice, also called *hexagonal-P* and often abbreviated by *hex*, is described by two lattice vectors $\underline{R}_1^{hex}$, $\underline{R}_2^{hex}$ of equal length a, forming an angle of either 120° (*obtuse representation*) or 60° (*acute representation*) with a third lattice vector $\underline{R}_3^{hex}$ of length c, which is perpendicular to both $\underline{R}_1^{hex}$ and $\underline{R}_2^{hex}$. Thus, the vectors of the obtuse representation can be described in Cartesian coordinates by

$$\underline{R}_1^{hex} = a(1, 0, 0), \quad \underline{R}_2^{hex} = a(-1/2, \sqrt{3}/2, 0), \quad \underline{R}_3^{hex} = c(0, 0, 1) \tag{2.37a}$$

and those of the acute representation by

$$\underline{R}_1^{hex} = a(1, 0, 0), \quad \underline{R}_2^{hex} = a(1/2, \sqrt{3}/2, 0), \quad \underline{R}_3^{hex} = c(0, 0, 1) \tag{2.37b}$$

where a and c are the lattice constants of the hexagonal lattice. While the two representations are equivalent, the obtuse representation of crystal lattices is often preferred to the acute one and will be used in the following.

There is a special type of crystal structure with hexagonal lattice, the so-called *hexagonal close-packed* (*hcp*) crystal structure. While its definition is theoretical in nature it occurs, to a good approximation, for many single crystals of metals, such as beryllium, magnesium, titanium, cobalt, or cadmium (Table E.3). The hcp crystal structure (Figure 2.10) is defined by a hexagonal lattice with a lattice constant ratio c/a of $\sqrt{(8/3)} = 1.63299$ and will be called *hex* (*hcp*) in the following. Further, the hexagonal unit cell of an hcp crystal contains two atoms (Figure 2.10b). The c/a ratio and the atom positions are chosen such that each atom is surrounded by 12 nearest-neighbor atoms at equal distance (equal to lattice constant a), achieving the same atom density as crystals with a corresponding fcc lattice.

Analogous to the family of cubic lattices, there is also a close connection between trigonal and hexagonal lattices, where scientists often prefer hexagonal lattice descriptions to trigonal ones. The *trigonal* lattice, also called *trigonal-R* or *rhombohedral*, is described by three lattice vectors $\underline{R}_1$, $\underline{R}_2$, $\underline{R}_3$ of equal length a, which also form identical angles $\alpha = \beta = \gamma$. Thus, the lattice vectors can be thought of as arising from each other by a 120° rotation about a common axis given by $(\underline{R}_1 + \underline{R}_2 + \underline{R}_3)$